RSC Advances

PAPER

View Article Online
View Journal | View Issue

Cite this: *RSC Adv.*, 2021, **11**, 13274

Bimetallic aluminum complexes bearing novel spiro-phenanthrene-monoketone/OH derivatives: synthesis, characterization and the ring-opening polymerization of ε-caprolactone†

Erlin Yue,[a] Furong Cao,[b] Jun Zhang,[c] Wenjuan Zhang,*[b] Youshu Jiang,[c] Tongling Liang[c] and Wen-Hua Sun*[c]

Received 17th February 2021
Accepted 23rd March 2021

DOI: 10.1039/d1ra01288f

rsc.li/rsc-advances

A series of spiro-phenanthrene-monoketone/OH derivatives (**L1–L6**) were synthesized and fully characterized with $^{1}H/^{13}C$ NMR spectroscopy and elemental analyses. By treating ligands with $AlMe_3$, oxygen-bridged binuclear aluminum complexes (**Al1–Al6**) were isolated and characterized by $^{1}H/^{13}C$ NMR spectroscopy. The molecular structures of ligands (**L2**, **L4** and **L5**) and complex **Al1** were determined by single crystal X-ray diffraction. In the presence of benzyl alcohol (BnOH), these aluminum complexes demonstrated high efficiency towards the ring-opening polymerization of ε-caprolactone (ε-CL), resulting in PCL in a linear manner with the BnO-end group. In addition, complexes **Al1** and **Al5** exhibited good catalytic activities even without BnOH. Moreover, complexes **Al3** and **Al6** with the bulkier substituent of ^{i}Pr at the *ortho*-position of the arylamines demonstrated better catalytic activities than the analogs. Moreover, substituents on the backbone also affected catalytic behaviors.

Introduction

Biodegradable polyesters, such as polylactides (PLA) and polycaprolactone (PCL), have attracted much attention due to their biodegradability, biocompatibility and permeability, and have been extensive biomaterials in the pharmaceutical industries over the past few decades.[1] These polyesters are commonly prepared by the ring-opening polymerization (ROP) of cyclic esters, such as ε-caprolactone (ε-CL) or lactide, and catalyzed by metal complexes as prevalent catalysts.[2] Aluminum complex catalysts[3] have appealed with good activities and being nicely characterized by NMR spectra in order to illustrate the coordination mechanism of the ROP of cyclic esters.[4] Beyond ε-CL, the stereoselective ROP of *rac*-lactides was first achieved using the salen–Al complex catalyst.[5] In general, the modifications of ligands with different substituents changed the steric and electronic environment around the metal in their aluminum complexes, thus finely tuning their activities and controllability of ROP.[6] Attractive aluminum catalysts for ROP of cyclic esters were derived from simply N^O bidentate ligands, in which the six-membered ring N^O bidentate aluminum complexes showed less activity than their five-membered ring analogs.[7] This was further confirmed by the DFT calculation, in which five-membered ring Al complexes reduced the steric repulsion and enhanced the activity of the ROP of ε-CL.[7] However, there were less examples of five-membered coordinated ring Al complexes than popular six-membered ring N^O bidentate aluminum complexes.[7–9]

The N^O bidentate aluminum complexes (A, Chart 1) with five-membered ring coordination were verified to be in monomeric or dimeric forms that depended on the bulkiness of Al–R,[10] but usually formed dimeric ones (B, Chart 1) derived from 2-(1,3,5-dithiazinan-5-yl)ethanols,[11] as well as other alcohols (C and D, Chart 1).[12] Notably, complex D could catalyze the cycloaddition of CO_2 with epoxies.[12b] The anilinotropone-based dimeric aluminum complexes (E) demonstrated high activities in the ring-opening polymerization (ROP) of *rac*-lactides with the assistance of BnOH.[13] Subsequently, dimeric aluminum complexes (F) initiated the ROP of ε-CL[14] with good controllability. Meanwhile, complexes G exhibited good activity for the ROP of cyclic esters, and reflected the polymerization mechanism through NMR measurements.[15]

[a]*Yan'an Key Laboratory of New Energy & New Functional Materials, Shaanxi Key Laboratory of Chemical Reaction Engineering, School of Chemistry and Chemical Engineering, Yan'an University, Yan'an 716000, China. E-mail: yueerlin@yau.edu.cn*

[b]*Beijing Key Laboratory of Clothing Materials R&D and Assessment, Beijing Engineering Research Center of Textile Nanofiber, School of Materials Science and Engineering, Beijing Institute of Fashion Technology, Beijing 100029, China. E-mail: zhangwj@bift.edu.cn*

[c]*Key Laboratory of Engineering Plastics and Beijing National Laboratory for Molecular Sciences, Institute of Chemistry, Chinese Academy of Sciences, Beijing 100190, China. E-mail: whsun@iccas.ac.cn*

† Electronic supplementary information (ESI) available: Details of crystallography and hydrogen bonding interactions of ligands. CCDC 2063065 (**L2**), 2063064 (**L4**), 2063180 (**L5**) and 2063066 (**Al1**). For ESI and crystallographic data in CIF or other electronic format see DOI: 10.1039/d1ra01288f

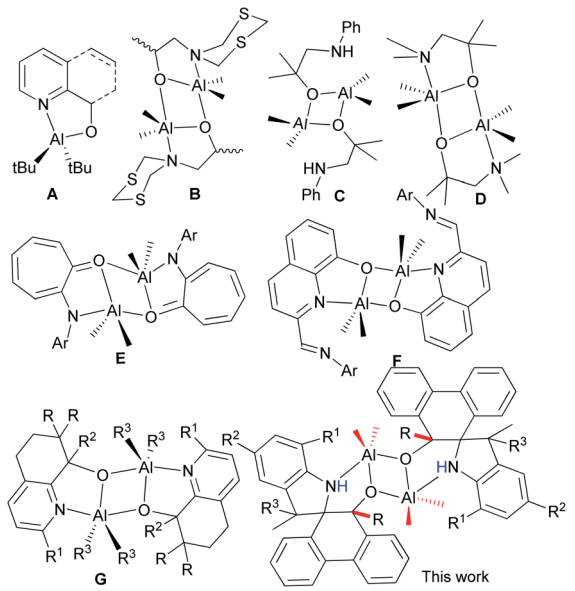

Chart 1 N^O bidentate aluminum complexes.

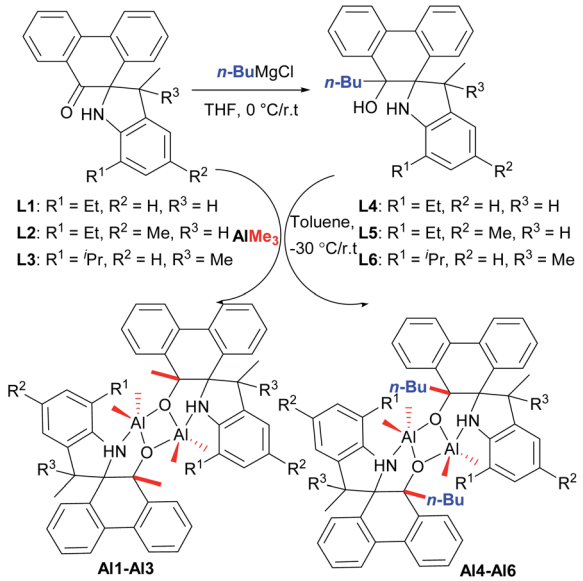

Scheme 1 Synthesis of the spiro-phenanthrene-mono–OH derivatives L4–L6 and aluminum complexes Al1–Al6.

Phenanthrene-based ligands were widely used to coordinate with transition metals,[16] and their metal complexes exhibited good activities for isoprene polymerization,[17] as well as coupling reactions.[18] However, there were a few examples with main group complexes, but with 9,10-diamido-phenanthrene only.[19] Phenanthrenequinone derivatives react extensively with trimethylaluminum, forming novel dimeric aluminum complexes bearing spiro-phenanthrene derivatives. Interestingly, these complexes show high activities towards the ring-opening polymerization of ε-caprolactone. Herein, the synthesis and characterization of the title complexes are reported, along with their catalytic performances towards the ROP of ε-CL.

Results and discussion

Synthesis and characterization of the ligands (L1–L6) and aluminum complexes (Al1–Al6)

According to our previous work,[18] refluxing the mixture of 9,10-phenanthrenequinone with various substituted anilines in the presence of *p*-toluenesulfonic acid (*p*-TsOH) in toluene afforded a series of novel spiro-phenanthrene-monoketone derivatives (**L1–L3**). Furthermore, the reduction reaction of **L1–L3** with *n*-BuMgCl gave the corresponding spiro-phenanthrene-mono–OH compounds (**L4–L6**) (Scheme 1). Treatment of ligands **L1–L6** with one equivalent of $AlMe_3$ in toluene at −30 °C gave the dialkylaluminum complexes (**Al1–Al6**), respectively, in acceptable yields (Scheme 1). For the preparation of **Al1–Al3**, one methyl group from $AlMe_3$ was added to the carbonyl (C=O). For the preparation of **Al1–Al6**, the elimination of CH_4 from the reaction between Al–Me and –OH occurred. All of these organic compounds and aluminum complexes were characterized by $^1H/^{13}C$ NMR spectroscopy and elementary analysis. Comparing the $^1H/^{13}C$ NMR spectra of the ligands, the disappearance of the –C=O resonance of **L1–L3** and the –OH resonance of the **L4–L6** in those of the corresponding aluminum complexes indicated the formation of the aluminum complexes. It is noteworthy that the resonance of –NH for all aluminum complexes **Al1–Al6** still remained, being similar to the reports of the –NH presence in aluminum complexes.[8,12a] Moreover, the crystal structures of the organic compounds **L2**, **L4** and **L5** and aluminum complex **Al1** were determined by single crystal X-ray diffraction (Fig. 1–4).

Suitable crystals of the organic compounds **L2**, **L4** and **L5** were readily achieved from their respective heptane solution,

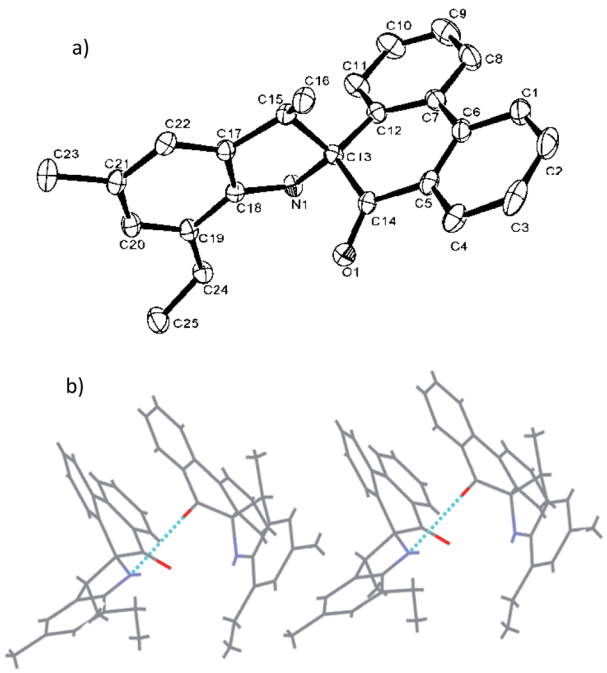

Fig. 1 (a) ORTEP drawing of L2. Thermal ellipsoids are shown at the 50% probability level. Hydrogen atoms have been omitted for clarity. (b) Hydrogen bonding motifs in L2.

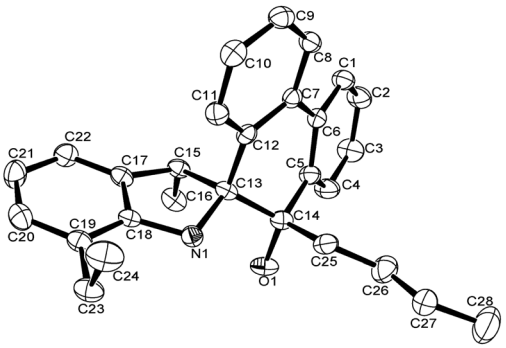

Fig. 2 ORTEP drawing of **L4**. Thermal ellipsoids are shown at the 50% probability level. Hydrogen atoms have been omitted for clarity.

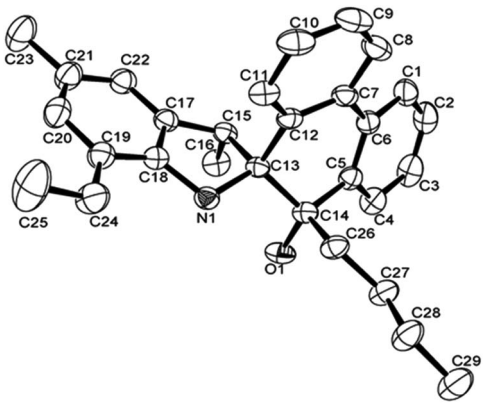

Fig. 3 ORTEP drawing of **L5**. Thermal ellipsoids are shown at the 50% probability level. Hydrogen atoms have been omitted for clarity.

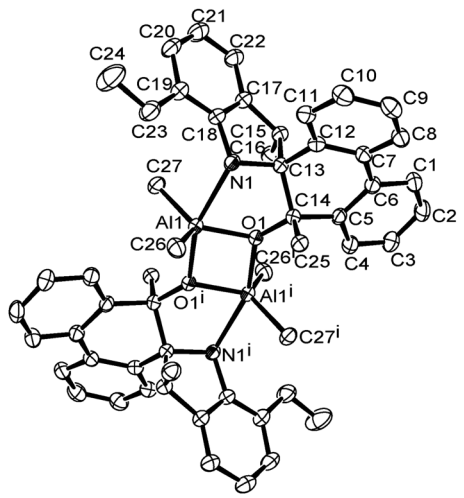

Fig. 4 ORTEP drawing of **Al1**. Thermal ellipsoids are shown at the 50% probability level. Hydrogen atoms and free solvent molecules have been omitted for clarity.

and were determined by means of single crystal X-ray diffraction (see Fig. 1–3). Selected bond lengths and bond angles are given in Table 1.

Table 1 Selected bond lengths (Å) and angles (°) for **L2**, **L4** and **L5**

	L2	**L4**	**L5**
Bond lengths (Å)			
N1–C13	1.467 (4)	1.487 (4)	1.4815 (16)
N1–C18	1.395 (4)	1.416 (4)	1.4221 (18)
O1–C14	1.218 (4)	1.427 (4)	1.4228 (16)
C13–C12	1.515 (5)	1.536 (4)	1.5356 (18)
C13–C14	1.536 (4)	1.557 (4)	1.5513 (19)
C13–C15	1.591 (5)	1.583 (4)	1.5818 (18)
C15–C16	1.525 (5)	1.537 (4)	1.5304 (19)
C15–C17	1.522 (5)	1.512 (4)	1.506 (2)
C17–C18	1.391 (5)	1.392 (4)	1.3917 (19)
Bond angles (°)			
C13–N1–C18	108.9 (3)	107.7 (2)	105.86 (10)
N1–C13–C12	112.8 (3)	112.7 (2)	112.06 (11)
N1–C13–C14	109.7 (3)	109.7 (2)	110.92 (10)
N1–C13–C15	102.8 (3)	102.5 (2)	102.75 (10)
N1–C18–C17	111.1 (3)	110.3 (3)	110.38 (12)
O1–C14–C5	122.4 (3)	108.0 (2)	107.02 (11)
O1–C14–C13	120.3 (3)	110.3 (3)	111.32 (11)

Fig. 1 shows the structure of **L2**, in which the five-membered rings are each constructed by C13, C15, C17–C18 and N1, and the O1–C14 bond length of **L2** is 1.218 (4) Å, indicating a typical double-bond character of C=O. The O atom deviated from the plane of spiro-phenanthrene (C6, C2, C4, C10, C11, C8) with a distance of 0.505 Å. The plane of the aryl ring (C7, C21, C19) is almost perpendicular to the spiro-phenanthrene plane with a dihedral angle of 78.14°. From the packing model, there was hydrogen bonding of N–H···O between two adjacent molecules. In addition, the plane of spiro-phenanthrene is almost parallel to another phenanthrene from adjacent molecules with a small dihedral angle of 8.07°.

The structures of **L4** and **L5** are shown in Fig. 2 and 3 and they are similar to **L2**. Both possessed the five-membered rings that were constructed by C13, C15, C17–C18 and N1. However, the bond lengths of O1–C14 in **L4** (1.427 (4) Å) and **L5** (1.4228 (16) Å) are much longer than that of **L2** (1.218 (4) Å), indicating the typical single bond characters. In addition, the bond length of N–C13, N–C18 in **L4** (1.487 (4), 1.416 (4) Å), **L5** (1.4815 (16), 1.4221 (18) Å) are much longer than that in **L2** (1.467 (4), 1.395 (4) Å), indicating the influence of the alkyl group on C14. Due to the more distorted six-membered ring, the dihedral angle between the two phenyl rings of phenanthrene is about 19.7°, but these two phenyl rings are almost particular to the aryl ring with a dihedral angle of 76.69 and 84.1°, respectively. There were also intermolecular hydrogen bonds in the ligands **L4** and **L5**, respectively, which came from O1–H1···N1. The motifs of hydrogen bonding are illustrated in Fig. S1 and S2.†

A single crystal of complex **Al1** suitable for the X-ray diffraction analysis was obtained from its toluene solution. The molecular structure of complex **Al1** is shown in Fig. 4, and the selected bond lengths and bond angles are collected in Table 2.

Table 2 Selected bond lengths (Å) and angles (°) for **Al1**

Bond lengths (Å)		Bond angles (°)	
Al1–O1	1.8669 (15)	O1–Al1–O1^{i}	79.51 (5)
Al1–O1^{i}	1.9881 (13)	O1–Al1–N1	79.59 (5)
Al1–N1	2.3291 (15)	O1^{i}–Al1–N1	159.10 (5)
Al1–C26	1.9960 (18)	O1–Al1–C26	115.68 (7)
Al1–C27	1.9813 (17)	O1–Al1–C27	122.84 (7)
O1–Al1^{i}	1.9882 (13)	O1^{i}–Al1–C26	100.96 (6)
O1–C14	1.4504 (18)	O1^{i}–Al1–C27	100.87 (7)
N1–C13	1.490 (2)	C26–Al1–C27	120.09 (8)
N1–C18	1.4388 (19)	N1–Al1–C26	88.41 (6)
Al1–Al1^{i}	2.9647 (15)	N1–Al1–C27	90.18 (7)

Fig. 4 shows the complex **Al1** as a dimeric form, which is symmetrically penta-coordinated by two bridged oxygen atoms (O1 and O1^{i}), one nitrogen atom (N1) from the spiro-phenanthrene-monoketone ligand and two coordinating methyl anions from the trimethylaluminum. Each aluminum possessed a distorted trigonal bipyramidal geometry. Another methyl anion from trimethylaluminum was added to the carbonyl of the spiro-phenanthrene-monoketone ligand. Complex **Al1** possessed a C_2 symmetric axis through the centroid of the Al1–O1–Al^{i}–O1^{i} plane. However, there is a slight asymmetry in the Al_2O_2 four-membered ring system. The bond lengths of the Al1–O1 [1.8669 (15) Å] and Al1–N1 [2.3291 (15) Å] in **Al1** are shorter than the corresponding ones in the dimethylaluminum 2-chloro-6,6-dimethylcyclopentyl-pyridin-7-oxylates [1.8735 (14) Å, 2.3500 (17) Å].[15c] The quadrilateral center comprises Al1, O1, Al1^{i} and O1^{i}, but there is no direct bonding between the two aluminum atoms with an intramolecular distance of 2.9647 (15) Å. The dihedral angle between the two phenyl rings of spiro-phenanthrene is about 27.29°, much larger than that in **L2**, indicating the greater distortion of the six-membered ring after coordination with Al. In addition, although N–H remained in the **Al1** complex, there was no hydrogen bonding observed in **Al1** due to the bulky environment around the N atom.

Ring-opening polymerization of ε-CL catalyzed by Al complexes Al1–Al6

First, complex **Al1** was evaluated for the ring opening polymerization of *rac*-LA under various conditions, but there was no polymer product. In contrast, the ROP of ε-CL proceeded smoothly. Therefore, the ring opening polymerization of ε-CL was investigated in detail, and the polymerization results are collected in Table 3. The complex **Al1** was employed to study the effect of temperature, molar ratio, and reaction time on the ROP of ε-CL. The results showed that there was no polymer observed at room temperature or 30 °C when the ROP of ε-CL was conducted at a molar ratio [CL] : [Al] : [BnOH] of [250 : 1 : 1]. When increasing the temperature from 60 °C to 90 °C (Table 3, runs 1–3), the polymer yield with 30 minutes gradually increased from 3% to 45%. Further increasing the temperature to 100 °C led to a significant increase of the polymer yield (up to 93%) (Table 3, run 4). This temperature effect on the polymerization agreed well with our previous results, in which the mononuclear species is proposed as the real active species for the ring opening polymerization of ε-CL and the ratio of the mononuclear species increased at higher temperature (verified by ^{27}Al NMR).[15b] However, a higher temperature of 110 °C resulted in a quick decrease of yield (64%, run 5, Table 3). The higher monomer ratio led to a slight decrease of the polymer yield and increase of the molecular weight. Prolonging the reaction time from 10 minutes to 60 minutes led to the gradual increase of yields from 89% to almost 100%. At the same time, the molecule weights are quite similar (4.28–4.86 $\times$ 10^4 g mol^{-1}), indicating the minimal effect of the reaction time. Without BnOH, **Al1** still exhibited good efficiency for ROP of ε-CL with 87% polymer yield, but producing the PCL with high molecular weight (8.95 $\times$ 10^4 g mol^{-1}). When two equivalents of BnOH were used, the polymer yield was kept at 85%. However, the molecular weight sharply decreased from 8.95 to 2.55 $\times$ 10^4 g mol^{-1}, indicating the significant chain transfer of BnOH (runs 4, 11 and 12, Table 3).

Considering the potential role of the long chain of the butyl group on improving the polymerization activity or molecular weight of PCL, **Al5** was also investigated for ROP under the same condition. The results showed that without BnOH, the molecular weight of the polymer by **Al5** was much higher than that by **Al1** (run 13 *vs.* 11, Table 3), up to 12.4 $\times$ 10^4 g mol^{-1}. When increasing the BnOH amount, the polymer yield did not change a lot. However, the molecular weight of PCL sharply decreased (runs 13–15, Table 3), also indicating the chain transfer of BnOH. In the presence of BnOH, the polymerizations were conducted at various temperatures and the highest yield was achieved at 100 °C. In prolonging the reaction time from 30 min to 60 minutes, the polymer yield gradually increased from 83% to 95%. However, upon increasing the monomer molar ratio from 250 to 400 and 500, the polymer yield dramatically decreased from 83% to 31% and 0% (runs 20–22, Table 3). It is probable that the deactivation of the complexes by impurities in the monomer account for this.

At 100 °C and with the molar ratio of [CL] : [Al] as 250 within 30 minutes, all other aluminum complexes were investigated for ROP of ε-CL. The results showed that the polymer yields by **Al1–Al6** bearing the *n*-Bu group are generally lower than those by **Al1–Al3** having the methyl group, which was demonstrated by the yield order: **Al4** < **Al1**, **Al5** < **Al2**, **Al6** < **Al3**, indicating a steric effect of the bulkier substituent around the Al center. In addition, the R^2 group has a small effect on the polymer yield, which was demonstrated by the same order of polymer yield: **Al3** (R^2 = H) > **Al1** (R^2 = H) > **Al2** (R^2 = Me); **Al6** (R^2 = H) > **Al4** (R^2 = H) > **Al5** (R^2 = Me). The reason is probably due to the stronger electron donor ability of methyl group.

The obtained PCL was characterized by ^{1}H NMR and MALDI-TOF spectra (shown in Fig. 5). ^{1}H NMR clearly showed the signal of PhCH$_2$O (7.35, 5.11 ppm), indicating the active species of Al–OCH$_2$Ph in the polymerization process. The MALDI-TOF spectrum of the polymer also showed that there was one major family in the product (Fig. 5), in which the interval 114.2 Da was observed between the adjacent peaks (one repeat unit of polymer), and it can be ascribed to PhCH$_2$O + 114.1 $\times$ *n* (number of

Table 3 The ROP of ε-CL catalyzed by complexes **Al1–Al6**.[a]

Run	Cat.	CL : Al : BnOH	T/°C	t/min	Isolated yields[b] (%)	M_n[c]c ($\times 10^4$)	M_{ncald} ($\times 10^4$)[d]	PDI[c]c
1	**Al1**	250 : 1 : 1	60	30	3	1.10	0.10	1.32
2	**Al1**	250 : 1 : 1	80	30	26	2.05	0.75	1.44
3	**Al1**	250 : 1 : 1	90	30	45	1.86	1.29	1.67
4	**Al1**	250 : 1 : 1	100	30	93	4.37	2.66	1.41
5	**Al1**	250 : 1 : 1	110	30	64	3.27	1.83	1.33
6	**Al1**	400 : 1 : 1	100	30	85	5.48	3.89	1.39
7	**Al1**	250 : 1 : 1	100	10	89	4.71	2.55	1.34
8	**Al1**	250 : 1 : 1	100	20	91	4.28	2.60	1.51
9	**Al1**	250 : 1 : 1	100	40	96	4.54	2.75	1.38
10	**Al1**	250 : 1 : 1	100	60	>99	4.86	2.86	1.36
11	**Al1**	250 : 1 : 0	100	30	87	8.95	—	1.89
12	**Al1**	250 : 1 : 2	100	30	85	2.55	1.22	1.19
13	**Al5**	250 : 1 : 0	100	30	81	12.45	—	1.87
14	**Al5**	250 : 1 : 1	100	30	83	2.82	2.38	1.47
15	**Al5**	250 : 1 : 2	100	30	71	2.70	1.02	1.24
16	**Al5**	250 : 1 : 1	80	30	36	2.92	1.04	1.39
17	**Al5**	250 : 1 : 1	90	30	67	4.05	1.92	1.31
18	**Al5**	250 : 1 : 1	110	30	48	2.15	1.38	1.86
19	**Al5**	250 : 1 : 1	100	40	87	1.99	2.49	1.70
20	**Al5**	250 : 1 : 1	100	60	95	2.16	2.72	2.04
21	**Al5**	400 : 1 : 1	100	30	31	1.56	1.42	1.96
22	**Al5**	500 : 1 : 1	100	30	0	—	—	—
23	**Al2**	250 : 1 : 1	100	30	77	3.34	2.21	1.31
24	**Al3**	250 : 1 : 1	100	30	96	4.42	2.75	1.34
25	**Al4**	250 : 1 : 1	100	30	85	4.27	2.43	1.31
26	**Al6**	250 : 1 : 1	100	30	86	1.91	2.46	1.70

[a] Conditions: 20 μmol Al; 1.0 M ε-CL toluene solution. [b] Isolated yield: weight of the polymer obtained/weight of monomer used. [c] GPC data in THF *vs.* polystyrene standards, using a correcting factor of 0.56.[20] [d] M_n (calcd) = (monomer/initiator) × (conversion) × 114 + 108 (M_w of BnOH).

repeat units) + Na^+, a typical character of the linear structure, which agrees well with its ^1H NMR spectrum.

Conclusion

The oxygen-bridged binuclear aluminum complexes (**Al1–Al6**) bearing spiro-phenanthrene-monoketone/OH derivatives (**L1–L6**) were prepared and fully characterized by $^1H/^{13}C$ NMR spectroscopy, elemental analyses and single crystal X-ray diffraction. The crystal structure of **Al1** indicated an oxygen-bridged dimeric form in the solid state. All aluminum complexes demonstrated moderate to high efficiency for the ROP of ε-caprolactone (ε-CL) in the presence of benzyl alcohol (BnOH), producing the linear PCL capped with the BnO. The complexes **Al3** and **Al6** containing bulkier ^{i}Pr substitutes at the *ortho*-position of arylamine can enhance the catalytic activities for the ROP of ε-CL. More importantly, the complexes **Al1** and **Al5** also exhibited good catalytic activities in the absence of BnOH.

Experimental section

General consideration

All manipulations involving air- and moisture-sensitive compounds were performed using standard Schlenk techniques under a nitrogen atmosphere. Toluene was refluxed over

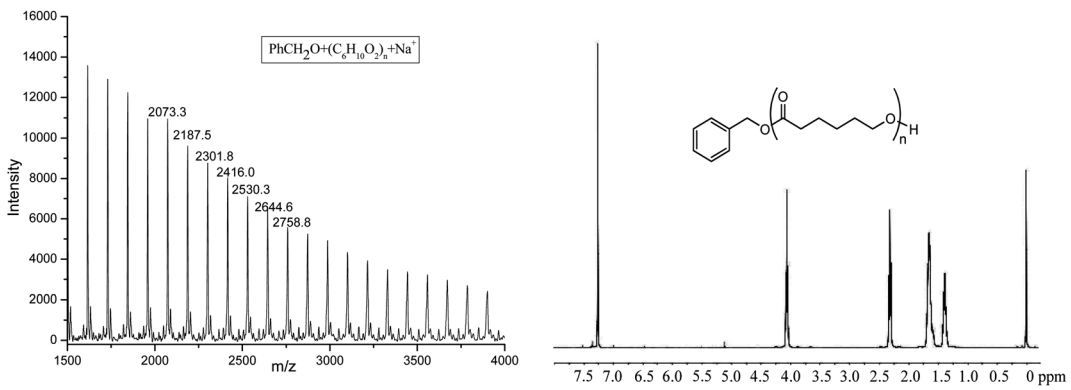

Fig. 5 The MALDI-TOF spectrum and ^1H NMR of PCL obtained by **Al1** + BnOH (run 4, Table 3).

sodium and distilled under nitrogen prior to use. Other reagents were purchased from Aldrich, Acros, or local suppliers. NMR spectra were recorded on a Bruker DMX 400 MHz instrument at ambient temperature using TMS as an internal standard; δ values were given in ppm and J values in Hz. ^{1}H NMR spectra are referenced using the residual solvent peak at δ 7.26 ppm for $CDCl_3$ and δ 7.16 ppm for C_6D_6. ^{13}C NMR spectra are referenced using the residual solvent peak at 77.16 ppm for $CDCl_3$ and δ 128.06 ppm for C_6D_6. Elemental analysis was carried out using a Flash EA 1112 micro-analyzer. Molecular weights and the molecular weight distribution (MWD) of polyethylene were determined by PL-GPC220 at room temperature, with tetrahydrofuran (THF) as the solvent. The compounds spiro-[7-ethyl-3-methylindoline-2,10-phenanthren-9-one] (**L1**)[18] and spiro-[7-isopropyl-3,3-dimethylindoline-2,10-phenanthren-9-one] (**L3**)[16c] were prepared according to the reported literature.

Synthesis of phenanthrene-based ligands

Spiro-[5-methyl-7-ethyl-3-methylindoline-2,10-phenanthren-9-one] (L2). A 100 mL toluene solution of 9,10-phenanthrenequinone (2.00 g, 9.61 mmol), 2,6-diethyl-4-methylphenylamine (3.14 g, 19.2 mmol), and a catalytic amount of *p*-toluenesulfonic acid (0.365 g, 1.92 mmol) was refluxed for 8 h. The solvent was evaporated under reduced pressure, and the mixture was then purified by silica gel column chromatography with petroleum ether/ethyl acetate (v/v = 100 : 1) as the eluent. It was then recrystallized in heptane to afford the product as a yellow powder (0.966 g) in 28% yield. ^{1}H NMR (400 MHz, $CDCl_3$, 25 °C): δ 7.97 (d, J = 8.0 Hz, 1H), 7.91–7.87 (m, 2H), 7.77–7.75 (m, 1H), 7.70–7.66 (m, 1H), 7.43–7.29 (m, 3H), 6.85 (s, 1H), 6.57 (s, 1H), 4.59 (s, 1H), 3.45–3.39 (m, 1H), 2.75–2.65 (m, 2H), 2.25 (s, 3H), 1.37 (d, J = 7.2 Hz, 3H), 0.97 (d, J = 7.2 Hz, 3H). ^{13}C NMR (100 MHz, $CDCl_3$, 25 °C): δ 201.5, 146.2, 143.1, 137.6, 134.7, 131.4, 131.3, 130.0, 129.9, 129.5, 128.6, 128.1, 128.0, 127.2, 127.0, 126.5, 124.2, 123.1, 121.8, 77.6, 54.7, 24.5, 21.1, 17.8, 13.8. Anal. calcd for $C_{25}H_{23}NO$: C, 84.95; H, 6.56; N, 3.96. Found: C, 84.67; H, 6.36; N, 4.01.

Spiro-[7-ethyl-3-methylindoline-2,10-phenanthren-9-*n*-butyl-9-hydroxyl] (L4). Under a nitrogen atmosphere, the ligand **L1** (1.00 g, 2.95 mmol) was dissolved in 30 mL THF, and then added to a solution of *n*-BuMgCl (4.4 mL, 1.0 M) in an ice bath. The mixture was stirred overnight, and then quenched by saturated ammonium chloride with stirring and extracted with CH_2Cl_2 (20 mL × 3). The combined organic layers were dried over anhydrous $MgSO_4$, concentrated under reduced pressure, recrystallized in heptane and dried in vacuum to obtain a white powder (0.973 g) in 83% yield. ^{1}H NMR (400 MHz, $CDCl_3$, 25 °C): δ 7.74–7.67 (m, 3H), 7.41–7.27 (m, 3H), 7.13 (t, J = 7.2 Hz, 1H), 7.06 (d, J = 7.6 Hz, 1H), 6.99 (d, J = 6.8 Hz, 1H), 6.76–6.70 (m, 2H), 4.14 (s, 1H), 3.19–3.14 (m, 1H), 2.75–2.70 (m, 1H), 2.65 (s, 1H), 1.47–1.39 (m, 5H), 1.12 (d, J = 7.2 Hz, 3H), 1.07–0.95 (m, 1H), 0.79–0.71 (m, 4H). ^{13}C NMR (100 MHz, $CDCl_3$, 25 °C): δ 146.7, 144.1, 140.0, 133.5, 133.2, 128.1, 127.7, 127.6, 127.5, 126.6, 126.3, 124.7, 124.4, 123.7, 122.8, 121.9, 120.2, 77.4, 74.5, 50.4, 37.9, 25.8, 24.4, 23.1, 20.9, 14.3, 13.5. Anal. calcd for $C_{28}H_{31}NO$: C, 84.59; H, 7.86; N, 3.52. Found: C, 84.32; H, 7.92; N, 3.81.

Spiro-[5-methyl-7-ethyl-3-methylindoline-2,10-phenanthren-9-*n*-butyl-9-hydroxyl] (L5). In a manner similar to that described for **L4**, except for using **L2** instead of **L1**, **L5** was prepared as a white powder (0.515 g) in 44% yield. ^{1}H NMR (400 MHz, $CDCl_3$, 25 °C): δ 7.73–7.67 (m, 3H), 7.40–7.28 (m, 3H), 7.12 (t, J = 7.6 Hz, 1H), 7.03 (d, J = 7.6 Hz, 1H), 6.80 (s, 1H), 6.52 (s, 1H), 4.03 (s, 1H), 3.13–3.08 (m, 1H), 2.72–2.66 (m, 3H), 2.21 (s, 3H), 1.45–1.37 (m, 6H), 1.12–1.10 (m, 4H), 0.74–0.70 (m, 4H). ^{13}C NMR (100 MHz, $CDCl_3$, 25 °C): δ 144.4, 144.3, 140.1, 133.8, 133.2, 132.1, 129.8, 128.1, 127.7, 127.6, 127.5, 127.3, 126.3, 124.7, 124.4, 123.7, 122.7, 122.6, 77.4, 74.5, 50.4, 38.0, 25.8, 24.4, 23.1, 21.2, 21.1, 14.3, 13.6. Anal. calcd for $C_{29}H_{33}NO$: C, 84.63; H, 8.08; N, 3.40. Found: C, 84.25; H, 8.21; N, 3.58.

Spiro-[7-isopropyl-3,3-dimethylindoline-2,10-phenanthren-9-*n*-butyl-9-hydroxyl] (L6). In a manner similar to that described for **L4**, and using **L3** instead of **L1**, **L6** was prepared as a white powder (0.592 g) in 69% yield. ^{1}H NMR (400 MHz, $CDCl_3$, 25 °C): δ 7.68 (t, J = 7.6 Hz, 2H), 7.62–7.59 (m, 1H), 7.41–7.30 (m, 4H), 7.22–7.18 (m, 1H), 7.02 (d, J = 7.2 Hz, 1H), 6.75 (d, J = 7.2 Hz, 1H), 6.69 (d, J = 6.8 Hz, 1H), 4.23 (s, 1H), 3.07–3.00 (m, 1H), 2.27 (s, 3H), 1.58–1.54 (m, 2H), 1.42–1.38 (m, 6H), 1.13 (s, 3H), 1.10–0.92 (m, 2H), 0.71 (t, J = 7.2 Hz, 3H), 0.61 (s, 3H). ^{13}C NMR (100 MHz, $CDCl_3$, 25 °C): δ 145.0, 140.4, 140.0, 138.4, 134.6, 133.0, 128.1, 127.9, 127.8, 127.7, 127.5, 126.3, 125.6, 124.0, 123.9, 123.3, 119.7, 119.5, 79.5, 78.2, 50.2, 38.1, 29.7, 29.3, 27.8, 25.9, 23.1, 22.4, 14.2. Anal. calcd for $C_{30}H_{35}NO$: C, 84.66; H, 8.29; N, 3.29. Found: C, 84.45; H, 8.31; N, 3.42.

Synthesis of aluminum complexes Al1–Al6

Synthesis of Al1. Into a stirred solution of compound **L1** (0.34 g, 1.0 mmol) in toluene (10 mL), 1.0 mL $AlMe_3$ solution (1.0 M solution in toluene) was added dropwise in an ice-bath. The solution became red brown. The solution was allowed to warm slowly to room temperature, and was stirred for 24 h. The solvent was evaporated under reduced pressure. The residue was then added to 10 mL hexane and stirred for 1 h, filtering and washing with hexane to obtain a white powder (0.20 g) in a yield of 49%. ^{1}H NMR (400 MHz, C_6D_6, 25 °C): δ 8.40 (d, J = 8.0 Hz, 1H), 7.55 (d, J = 8.0 Hz, 1H), 7.50 (d, J = 8.0 Hz, 1H), 7.32 (t, J = 8.0 Hz, 1H), 7.22–7.19 (s, 1H), 7.02 (t, J = 8.0 Hz, 1H), 6.86–6.74 (m, 3H), 6.66 (d, J = 8.0 Hz, 1H), 6.46 (d, J = 8.0 Hz, 1H), 5.04 (s, 1H, NH), 3.20–3.14 (m, 1H), 2.55–2.50 (m, 2H), 1.59 (s, 3H), 1.40 (d, J = 8.0 Hz, 3H), 1.19 (t, J = 8.0 Hz, 3H), −0.08 (s, 3H), −0.66 (s, 3H). ^{13}C NMR (100 MHz, C_6D_6, 25 °C): δ 145.9, 143.8, 141.7, 137.1, 134.4, 132.3, 130.1, 128.8, 127.6, 127.1, 126.5, 125.7, 125.6, 124.4, 123.5, 120.3, 79.7, 78.6, 50.9, 31.6, 24.3, 21.4, 13.6, −3.0, −8.2. Anal. calcd for $C_{54}H_{60}Al_2N_2O_2$: C, 78.80; H, 7.35; N, 3.40. Found: C, 78.45; H, 7.31; N, 3.57.

Synthesis of Al2. In a manner similar to that described for **Al1**, using **L2** instead of **L1**, **Al2** was prepared as a white powder (0.63 g) in 35% yield. ^{1}H NMR (400 MHz, C_6D_6, 25 °C): δ 8.41 (d, J = 8.0 Hz, 1H), 7.57 (d, J = 8.0 Hz, 1H), 7.51 (d, J = 8.0 Hz, 1H), 7.32 (t, J = 8.0 Hz, 1H), 7.21 (t, J = 8.0 Hz, 1H), 7.04 (d, J = 8.0 Hz, 1H), 6.79 (t, J = 8.0 Hz, 1H), 6.74 (s, 1H), 6.70 (s, 1H), 6.28 (s,

1H), 5.01 (s, 1H, NH), 3.20–3.14 (m, 1H), 2.56–2.50 (m, 2H), 1.97 (s, 3H), 1.59 (s, 3H), 1.43 (d, J = 8.0 Hz, 3H), 1.22 (t, J = 8.0 Hz, 3H), −0.07 (s, 3H), −0.62 (s, 3H). ^{13}C NMR (100 MHz, C_6D_6, 25 °C): 145.6, 143.2, 138.0, 137.2, 136.5, 134.0, 131.9, 130.3, 128.7, 128.2, 127.9, 127.7, 127.3, 125.7, 124.3, 124.2, 123.9, 119.8, 79.9, 77.4, 50.5, 31.6, 24.3, 21.4, 14.0, −5.2, −9.9. Anal. calcd for $C_{56}H_{64}Al_2N_2O_2$: C, 79.03; H, 7.58; N, 3.29. Found: C, 79.35; H, 7.41; N, 3.47.

Synthesis of Al3. In a manner similar to that described for **Al1**, using **L3** instead of **L1**, **Al3** was prepared as a white powder (0.14 g) in 32% yield. ^{1}H NMR (400 MHz, C_6D_6, 25 °C): δ 8.34 (d, J = 8.0 Hz, 1H), 7.47 (d, J = 8.0 Hz, 2H), 7.29 (t, J = 8.0 Hz, 1H), 7.19 (d, J = 8.0 Hz, 1H), 7.03–6.88 (m, 3H), 6.79–6.74 (m, 2H), 6.50 (d, J = 8.0 Hz, 1H), 5.25 (s, 1H, NH), 3.13–3.03 (m, 1H), 1.69 (s, 3H), 1.66 (s, 3H), 1.32 (d, J = 8.0 Hz, 3H), 1.20 (d, J = 8.0 Hz, 3H), 0.66 (s, 3H), −0.13 (s, 3H), −0.67 (s, 3H). ^{13}C NMR (100 MHz, C_6D_6, 25 °C): δ 144.7, 142.0, 141.8, 138.8, 137.9, 136.4, 134.9, 133.8, 129.3, 125.7, 124.9, 124.7, 123.9, 122.0, 121.6, 83.3, 51.1, 34.7, 30.0, 29.7, 29.2, 24.2, 22.7, 21.4, −4.1, −8.7. Anal. calcd for $C_{58}H_{68}Al_2N_2O_2$: C, 79.24; H, 7.80; N, 3.19. Found: C, 79.45; H, 7.52; N, 3.24.

Synthesis of Al4. In a manner similar to that described for **Al1**, using **L4** instead of **L1**, **Al4** was prepared as a white powder (0.40 g) in 22% yield. ^{1}H NMR (400 MHz, C_6D_6, 25 °C): δ 8.81 (d, J = 7.6 Hz, 1H), 7.45 (d, J = 7.6 Hz, 1H), 7.37 (d, J = 7.6 Hz, 1H), 7.29 (t, J = 7.6 Hz, 1H), 7.14–7.11 (m, 1H), 7.06–7.01 (m, 1H), 6.96 (t, J = 7.6 Hz, 1H), 6.81–6.77 (m, 2H), 6.68 (t, J = 7.6 Hz, 1H), 6.53 (d, J = 7.6 Hz, 1H), 6.36–6.34 (m, 1H), 5.14 (s, 1H, NH), 3.10–3.04 (m, 1H), 2.46–2.40 (m, 2H), 2.11–1.99 (m, 2H), 1.95–1.79 (m, 2H), 1.32 (d, J = 7.6 Hz, 3H), 1.12 (d, J = 7.6 Hz, 3H), 0.91–0.82 (m, 2H), 0.69 (t, J = 6.8 Hz, 3H), −0.08 (s, 3H), −0.60 (s, 3H). ^{13}C NMR (100 MHz, C_6D_6, 25 °C): δ 142.0, 140.8, 136.4, 134.2, 132.4, 130.6, 129.3, 128.7, 128.6, 128.3, 127.5, 127.4, 125.7, 125.2, 123.5, 120.3, 79.4, 51.2, 41.3, 27.7, 24.4, 23.2, 23.1, 21.4, 14.0, 13.3, −1.95, −6.03. Anal. calcd for $C_{60}H_{72}Al_2N_2O_2$: C, 79.44; H, 8.00; N, 3.09. Found: C, 79.56; H, 7.82; N, 3.18.

Synthesis of Al5. In a manner similar to that described for **Al1**, using **L5** instead of **L1**, **Al5** was prepared as a white powder (0.89 g) in 47% yield. ^{1}H NMR (400 MHz, C_6D_6, 25 °C): δ 8.88 (d, J = 7.6 Hz, 1H), 7.49 (d, J = 7.6 Hz, 1H), 7.41 (d, J = 7.6 Hz, 1H), 7.33 (t, J = 7.2 Hz, 1H), 7.19 (d, J = 6.8 Hz, 1H), 7.00 (t, J = 7.6 Hz, 1H), 6.74 (t, J = 7.6 Hz, 1H), 6.70 (s, 1H), 6.61 (d, J = 7.6 Hz, 1H), 6.20 (s, 1H), 5.14 (s, 1H, NH), 3.12–3.07 (m, 1H), 2.50–2.44 (m, 2H), 1.97 (s, 3H), 1.38 (d, J = 7.6 Hz, 3H), 1.31–1.11 (m, 8H), 0.92 (t, J = 7.2 Hz, 3H), 0.72 (t, J = 6.8 Hz, 3H), −0.03 (s, 3H), −0.52 (s, 3H). ^{13}C NMR (100 MHz, C_6D_6, 25 °C): δ 142.2, 139.1, 138.3, 137.1, 136.5, 134.2, 132.5, 130.3, 128.7, 128.3, 127.8, 127.6, 125.7, 125.2, 124.2, 120.4, 79.6, 51.2, 41.4, 32.0, 27.8, 24.4, 23.2, 23.1, 21.4, 14.4, 14.0, 13.5, −1.94, −5.82. Anal. calcd for $C_{62}H_{76}Al_2N_2O_2$: C, 79.62; H, 8.19; N, 3.00. Found: C, 79.48; H, 8.22; N, 3.08.

Synthesis of Al6. In a manner similar to that described for **Al1**, using **L6** instead of **L1**, **Al6** was prepared as a white powder (0.22 g) in 11% yield. ^{1}H NMR (400 MHz, C_6D_6, 25 °C): δ 8.84 (d, J = 7.6 Hz, 1H), 7.48 (d, J = 7.6 Hz, 1H), 7.36 (d, J = 7.6 Hz, 1H), 7.29 (t, J = 7.6 Hz, 1H), 7.13–7.11 (m, 1H), 7.06–7.00 (m, 1H), 6.98 (t, J = 7.6 Hz, 1H), 6.82–6.78 (m, 2H), 6.69 (t, J = 7.6 Hz, 1H), 6.54 (d, J = 7.6 Hz, 1H), 6.38–6.33 (m, 1H), 5.12 (s, 1H, NH), 3.15–3.08 (m, 1H), 1.67 (d, J = 7.6 Hz, 6H), 1.32 (d, J = 6.4 Hz, 3H), 1.20 (d, J = 6.8 Hz, 3H), 0.65 (s, 3H), −0.05 (s, 3H), −0.58 (s, 3H). The ^{13}C NMR signals were not resolved due to the low signal to noise ratio. Anal. calcd for $C_{64}H_{80}Al_2N_2O_2$: C, 79.80; H, 8.37; N, 2.91. Found: C, 79.64; H, 8.34; N, 3.12.

General procedure for ε-caprolactone ring-opening polymerization

A typical ring-opening polymerization procedure of ε-CL in the presence of one equivalent of benzyl alcohol (Table 3, run 5) is presented as follows. The precatalyst **Al1** (0.0082 g, 0.020 mmol) was dissolved in 2 mL of toluene in a Schlenk flask at room temperature. To this mixture, benzyl alcohol (0.020 mmol) in toluene solution was added and stirred at room temperature for 5 min. Then, the flask was placed in a temperature-controlled oil bath preheated at 100 °C for 5 min, and ε-CL (0.571 g, 5.0 mmol) was injected. The polymerization was terminated by the addition of glacial acetic acid (*ca.* 0.2 mL) into the reaction mixture until the solution was stirred for the described amount of time. The resulting viscous solution was diluted with dichloromethane, and then transferred into a beaker containing cold methanol (100 mL) with stirring. The resultant polymer was collected on filter paper, and dried under reduced pressure to give a white solid.

X-ray crystallographic studies

Crystals of **L2**, **L4**, and **L5** suitable for X-ray diffraction analyses were obtained from their heptane solution at room temperature overnight. Crystals of the complex **Al1** suitable for the X-ray diffraction analyses were obtained from its toluene solution. X-ray studies were carried out on a Rigaku Saturn724 + CCD with graphite-monochromatic Mo Kα radiation (λ = 0.71073 Å) at 173 (2) K. Cell parameters were obtained by global refinement of the positions of all collected reflections. Intensities were corrected for Lorentz and polarization effects and empirical absorption. The structures were solved by direct methods and refined by full-matrix least squares on F^2. All hydrogen atoms were placed in calculated positions. Structure solution and refinement were performed by using the SHELXL-2014 package.[21] Within the structure refinement of complex **Al1**, there were free solvent molecules that had no influence on the geometry of the main compounds. Therefore, the SQUEEZE option of the crystallographic program *PLATON*[22] was used to remove these free solvents from the structure. Details of the X-ray structure determinations and refinements are provided in Table S1.† Details of the hydrogen-bonding interactions of ligands (**L2, L4** and **L5**) are listed in Table S2.†

Conflicts of interest

There are no conflicts to declare.

Acknowledgements

This work was supported by the National Natural Science Foundation of China (No. 51973005 and 21871275). Dr Yue also acknowledges the support of the Yan'an High-level Talents Special Foundation (No. 2019-33) and the Doctoral Scientific Research Startup Project of Yan'an University (No. YDBK2019-22).

References

1 (*a*) M. M. Reddy, S. Vivekanandhan, M. Misra, S. K. Bhatia and A. K. Mohanty, *Prog. Polym. Sci.*, 2013, **38**, 1653–1689; (*b*) I. Armentano, N. Bitinis, E. Fortunati, S. Mattioli, N. Rescignano, R. Verdejo, M. A. Lopez-Manchado and J. M. Kenny, *Prog. Polym. Sci.*, 2013, **38**, 1720–1747; (*c*) M. Singhvi and D. Gokhale, *RSC Adv.*, 2013, **3**, 13558–13568.

2 (*a*) A. Arbaoui and C. Redshaw, *Polym. Chem.*, 2010, **1**, 801–826; (*b*) J. Gao, D. Zhu, W. Zhang, G. A. Solan, Y. Ma and W.-H. Sun, *Inorg. Chem. Front.*, 2019, **6**, 2619–2652; (*c*) O. Santoro, X. Zhang and C. Redshaw, *Catalysts*, 2020, **10**, 800; (*d*) B. J. O'Keefe, M. A. Hillmyer and W. B. Tolman, *J. Chem. Soc., Dalton Trans.*, 2001, 2215–2224.

3 (*a*) Y. Wei, S. Wang and S. Zhou, *Dalton Trans.*, 2016, **45**, 4471–4485; (*b*) C. M. Thomas, *Chem. Soc. Rev.*, 2010, **39**, 165–173; (*c*) J. Lewiński and A. E. H. Wheatley, *Top. Organomet. Chem.*, 2013, **41**, 1–58.

4 P. Dubois, N. Ropson, R. Jérôme and P. Teyssié, *Macromolecules*, 1996, **29**, 1965–1975.

5 N. Spassky, M. Wisniewski, C. Pluta and A. Le. Borgne, *Macromol. Chem. Phys.*, 1996, **197**, 2627–2637.

6 (*a*) Z. Zhong, P. J. Dijkstra and J. Feijen, *Angew. Chem., Int. Ed.*, 2002, **41**, 4510–4513; (*b*) N. Nomura, R. Ishii, M. Akakura and K. Aoi, *J. Am. Chem. Soc.*, 2002, **124**, 5938–5939; (*c*) Z. Zhong, P. J. Dijkstra and J. Feijen, *J. Am. Chem. Soc.*, 2003, **125**, 11291–11298; (*d*) N. Nomura, R. Ishii, Y. Yamamoto and T. Kondo, *Chem.–Eur. J.*, 2007, **13**, 4433–4451; (*e*) X. Pang, R. Duan, X. Li and X. Chen, *Polym. Chem.*, 2014, **5**, 3894–3900; (*f*) X. Pang, R. Duan, X. Li, C. Hu, X. Wang and X. Chen, *Macromolecules*, 2018, **51**, 906–913; (*g*) P. Wang, X. Hao, J. Cheng, J. Chao and X. Chen, *Dalton Trans.*, 2016, **45**, 9088–9096; (*h*) L. Qin, Y. Zhang, J. Chao, J. Cheng and X. Chen, *Dalton Trans.*, 2019, **48**, 12315–12325.

7 C.-L. Lee, Y.-F. Lin, M.-T. Jiang, W.-Y. Lu, J. K. Vandavasi, L.-F. Wang, Y.-C. Lai, M. Y. Chiang and H.-Y. Chen, *Organometallics*, 2017, **36**, 1936–1945.

8 (*a*) S. Gesslbauer, R. Savela, Y. Chen, A. J. P. White and C. Romain, *ACS Catal.*, 2019, **9**, 7912–7920; (*b*) S. Gesslbauer, H. Cheek, A. J. P. White and C. Romain, *Dalton Trans.*, 2018, **47**, 10410–10414.

9 F.-J. Lai, L.-L. Chiu, C.-L. Lee, W.-Y. Lu, Y.-C. Lai, S. Ding, H.-Y. Chen and K.-H. Wu, *Polymer*, 2019, **182**, 121812.

10 (*a*) J. A. Francis, S. G. Bott and A. R. Barron, *J. Chem. Soc., Dalton Trans.*, 1998, 3305–3310; (*b*) J. A. Francis, S. G. Bott and A. R. Barron, *J. Organomet. Chem.*, 2000, **597**, 29–37.

11 J. C. Gálvez-Ruiz, H. Nöth and A. Flores-Parra, *Inorg. Chem.*, 2003, **42**, 7569–7578.

12 (*a*) S. Yoon, S. H. Kim, J. Heo and Y. Kim, *Inorg. Chem. Commun.*, 2013, **29**, 157–159; (*b*) S. H. Kim, S. Y. Han, J. H. Kim, Y. Y. Kang, J. Lee and Y. Kim, *Eur. J. Inorg. Chem.*, 2015, 2323–2329.

13 M. Li, M. Chen and C. L. Chen, *Polymer*, 2015, **64**, 234–239.

14 W.-H. Sun, M. Shen, W. J. Zhang, W. Huang, S. F. Liu and C. Redshaw, *Dalton Trans.*, 2011, **40**, 2645–2653.

15 (*a*) Q. Zhang, W. Zhang, N. M. Rajendran, T. Liang and W.-H. Sun, *Dalton Trans.*, 2017, **46**, 7833–7843; (*b*) Q. Zhang, W. Zhang, G. A. Solan, T. Liang and W.-H. Sun, *Polymers*, 2018, **10**, 764–782; (*c*) D. Zhu, L. Guo, W. Zhang, X. Hu, K. Nomura, A. Vignesh, X. Hao, Q. Zhang and W.-H. Sun, *Dalton Trans.*, 2019, **48**, 4157–4167.

16 (*a*) D. N. Nicolaides, K. E. Litinas, G. K. Papageorgiou and J. Stephanidou-Stephanatou, *J. Heterocycl. Chem.*, 1991, **28**, 139–143; (*b*) G. A. Abakumov, V. K. Cherkasov, N. O. Druzhkov, Y. A. Kurskii, G. K. Fukin, L. G. Abakumova and T. N. Kocherova, *Synth. Commun.*, 2006, **36**, 3241–3247; (*c*) L. D. Li, C. S. B. Gomes, P. T. Gomes, L. F. Veiros and S. Y. Kim, *ARKIVOC*, 2009, 95–111; (*d*) V. K. Cherkasov, N. O. Druzhkov, T. N. Kocherova, A. S. Shavyrin and G. K. Fukin, *Tetrahedron*, 2012, **68**, 1422–1426; (*e*) C. Dong, D. A. Dickie, W. A. Maio and T. A. Manz, *ACS Omega*, 2018, **3**, 16858–16865; (*f*) S. Roy, B. Sarkar, D. Bubrin, M. Niemeyer, S. Zalis, G. K. Lahiri and W. Kaim, *J. Am. Chem. Soc.*, 2008, **130**, 15230–15231; (*g*) L. Li, M. Jeon and S. Y. Kim, *J. Mol. Catal. A: Chem.*, 2009, **303**, 110–116; (*h*) S. Sa, M. Jeon and S. Y. Kim, *J. Mol. Catal. A: Chem.*, 2014, **393**, 263–271; (*i*) A. Anjum, S. Paswan, M. Kumar, H. Ali and R. K. Dubey, *Asian J. Chem.*, 2019, **31**, 943–950.

17 B. Gao, X. Luo, W. Gao, L. Huang, S.-M. Gao, X. Liu, Q. Wu and Y. Mu, *Dalton Trans.*, 2012, **41**, 2755–2763.

18 Q. Mahmood, E. Yue, W. Zhang, G. A. Solan, T. Liang and W.-H. Sun, *Org. Chem. Front.*, 2016, **3**, 1668–1679.

19 N. O. Druzhkov, G. G. Kazakov, A. S. Shavyrin, E. V. Baranov, E. N. Egorova, A. V. Piskunov and G. A. Abakumov, *Inorg. Chem. Commun.*, 2018, **90**, 92–96.

20 M. Save, M. Schappacher and A. Soum, *Macromol. Chem. Phys.*, 2002, **203**, 889–899.

21 (*a*) G. M. Sheldrick, *Acta Crystallogr., Sect. A: Found. Adv.*, 2015, **71**, 3–8; (*b*) G. M. Sheldrick, *Acta Crystallogr., Sect. C: Struct. Chem.*, 2015, **71**, 3–8.

22 A. L. Spek, *Acta Crystallogr., Sect. C: Struct. Chem.*, 2015, **71**, 9–18.